Journal of Translational Medicine

RESEARCH Open Access

PXD101 inhibits malignant progression and radioresistance of glioblastoma by upregulating GADD45A

Xiaohong Hu[1,2,3†], Peijun Zhou[1,2†], Xingzhi Peng[1,2], Yiting Ouyang[1,2], Dan Li[3], Xia Wu[2,4*] and Lifang Yang[1,2*]

Abstract

Histone deacetylase inhibitors (HDACis) have shown a significant antitumor effect in clinical studies, and PXD101 is a novel HDACi which can cross the blood–brain barrier. In this study, we showed that PXD101 could significantly inhibit the proliferation and invasion of glioblastoma (GBM) cells, while promoting their apoptosis and radiosensitivity. Furthermore, it was found that PXD101 exerted its antitumor function by upregulating the expression of the growth arrest and DNA damage inducible protein α (GADD45A). Mechanistically, PXD101 promoted the transcription of GADD45A by directly acetylating the histones H3 and H4, and GADD45A enhanced apoptosis and radiosensitivity through the activation of P38 in the GBM cells. In vivo experiments also showed that PXD101 combined with radiotherapy could significantly inhibit the growth of GBM. This study provides experimental evidence for application of the novel HDACi PXD101 in the treatment of GBM, as well as new molecular markers and potential intervention targets that may be used in preventing GBM malignant progression and radioresistance.

Introduction

Glioma, which is the most common intracranial malignant tumor originating from glial cells, is classified into four grades based on histopathological characteristics, with grades III and IV being high-grade gliomas [1]. Glioblastoma (GBM) is the most common high-grade glioma; it is characterized by a poor prognosis, with a median survival time of only 14.6 months and a 5-year survival rate of less than 5% [2]. At present, the main treatments for GBM include surgery, radiotherapy, and pharmacotherapy (typically chemotherapy with concomitant temozolomide; TMZ) [3]. However, most GBMs are resistant to radiotherapy and chemotherapy, resulting in recurrence [4]. Therefore, it is meaningful to investigate the methods that promote radiosensitivity in GBM treatment.

Histone acetylation modification is co-regulated by acetyltransferases (HATs) and deacetylases (HDACs),

†Xiaohong Hu and Peijun Zhou contributed equally to this work.

*Correspondence:
Xia Wu
aileenwu@csu.edu.cn
Lifang Yang
yanglifang@csu.edu.cn
[1]Department of Oncology, Key Laboratory of Carcinogenesis and Cancer Invasion of Ministry of Education, National Clinical Research Center for Geriatric Disorders, Xiangya Hospital, Central South University, Xiangya Road 110, Changsha 410078, China
[2]Cancer Research Institute, School of Basic Medicine Science, Central South University, Changsha 410078, China
[3]Institute of Molecular Medicine and Oncology, College of Biology, Hunan University, Changsha 410012, China
[4]Department of Pathology, The Second Xiangya Hospital, Central South University, Renmin Middle Road 174, Changsha 410011, China

which participate in gene transcription and play an important role in tumor development [5]. Studies have found that tumor suppressor genes in malignant tumors are often modified by deacetylation, leading to gene silencing. In GBM, HDAC4 deacetylated histone H3 in the p21 promoter to inhibit its transcription, which promoted malignant tumor progression [6]. HDAC SIRT2 deacetylated the C-terminal lysine residues of p73 to mediate its inactivation, which is essential for the proliferation and tumorigenicity of GBM cells [7]. Therefore, knocking down HDAC or using its inhibitor (HDACi) could re-establish normal histone acetylation patterns to inhibit the malignant progression of tumors [8]. HDACi LMK235 reduced the cell viability and colony formation of GBM cells and induced TUBA acetylation and autophagy [9]. DWP0016 activated the transcription and acetylation of tumor suppressor p53 in U251 glioblastoma cells, thereby inducing growth inhibition, cell cycle arrest, and apoptosis [10]. In addition, some studies have found that HDACi could participate in the regulation of tumor radioresistance. Scriptaid enhanced the radiosensitivity of human head and neck squamous cell carcinoma cells [11]. In colorectal cancer, SAHA combined with radiotherapy could delay tumor growth in mice compared with radiotherapy alone, suggesting that it could be an effective radiosensitizer [12]. These studies provide effective evidence for the improvement of the radiosensitivity of GBM from the perspective of acetylation modification.

PXD101 is a hydroxamic acid-derived pan-HDACi which has been approved by the FDA as a new antitumor drug [13]. Inhibition of HDACs by PXD101 indirectly promoted an anticancer therapeutic effect by provoking acetylated histone accumulation, re-establishing normal gene expressions in cancer cells, and stimulating other routes [14]. In thyroid cancer, PXD101 elevated acetylated histone 3, p21(Waf), and PARP, which induced apoptosis and inhibited cell growth [15]. In pancreatic cancer, PXD101 promoted the activation of the ROS–TAK1–AMPK signaling axis to induce apoptosis and growth inhibition [16]. In rhabdomyomas, PXD101 increased ROS accumulation, inhibited DNA damage repair, and induced G2 cell cycle arrest, thereby promoting radiosensitivity [17]. In glioma, PXD101 could upregulate the expression of the apoptosis-related genes puma, bim, chop, and p21, thereby inducing apoptosis of LN229 cells [18]. However, its role and its molecular mechanism in GBM radiosensitivity have not been elucidated.

In the present study, PXD101 was found to inhibit GBM cell proliferation and induce cell apoptosis and radiosensitivity in vivo and in vitro. Mechanistically, PXD101 could upregulate the expression of GADD45A by directly acetylating histone H3 and H4 and could further promote the phosphorylation activation of P38. These results indicated that PXD101 may be a new radiosensitizer for GBM.

Materials and methods

Cell culture and reagents

The human glial cells HEB and glioma grade I cells HS683 (ATCC: HTB-138) were cultured in 1640 medium (GIBCO BRL, Grand Island, NY) containing 10% fetal bovine serum (FBS) (Hyclone, South Logan, UT). The glioma grade III cells SW1088 (ATCC: HTB-12) and grade IV GBM cells U251, LN229 (ATCC: CRL-2611), LN229-luc (iCell-0125a, iCell Bioscience Inc, Shanghai, China), T98G (ATCC: CRL-1690), and SF295 were cultured in DMEM medium (GIBCO BRL) containing 10% FBS. PXD101 (S1085, Selleck Chemicals, Houston, TX) was dissolved in dimethyl sulfoxide (DMSO, HY-Y0320, MedChemExpress, Monmouth Junction, NJ).

siRNA and plasmid transfection

The siRNAs of GADD45A were designed and synthesized by Ribo Bio (Guangzhou, China). The sequence of siRNAs is listed in Table S1. The transfection of siRNA was carried out using Lipofectamine™ 3000 Transfection Reagent (L3000150, Thermo Fisher Scientific, Waltham, MA), according to the manufacturer's instructions. The Flag-HA-pcDNA3.1-vector plasmid (52535) and PGL3-basic vector (212936) plasmid were purchased from Addgene. After the Flag-HA-pcDNA3.1-vector plasmid was digested using Hind III-HF (R3104T, New England Biolabs, MA) and Xba I (R0145T, New England Biolabs), the GADD45A coding sequence was inserted into the vector to obtain the recombinant plasmids pcDNA-HA-GADD45A (GADD45A-OE) using a homologous recombination kit (C214, Vazyme, Nanjing, China). After the PGL3-basic vector was digested with Hind III-HF, the GADD45A promoter sequence was inserted into the vector to obtain the recombinant plasmids pGL3-basic-GADD45A-promoter. The homologous recombination primers are listed in Table S2. Neofect (TF201201, Neofect Biotech, Beijing, China) was used for plasmid transfection, according to the manufacturer's instructions.

Cell viability assay

Cell viability was analyzed using the MTS kit (G5421, Promega, Madison, US), according to the reagent manufacturer's instructions. The cells were cultured in 96-well plates for an appropriate time; the viability was measured as OD490 values after 2 h of incubation in a determination solution using a microplate reader (BioTek ELx800, Winooski, VT). Nonlinear regression analysis using GraphPad Prism software was used to determine the IC50 value.

Colony formation assay

Equal numbers of cells from the control group and treatment group were inoculated into a 6-well plate and further cultured for 14 days to form colonies. Subsequently, it was fixed with 4% paraformaldehyde and stained with crystal violet solution (219215, Sigma-Aldrich, St. Louis, US). The colonies were observed under a microscope (Olympus, Tokyo, Japan) and photographed.

Apoptosis assay

The cells were collected and stained with annexin V and propidium iodide (PI) using an apoptosis kit (KGA103, Keygen Biotech, Jiangsu, China), according to the manufacturer's instructions. The apoptosis ratio of the cells was analyzed using flow cytometry (Fortessa, BD Biosciences, San Jose, CA).

Scratch assay

The cells were seeded in 6-well culture plates and incubated overnight to a density of 70–80%. The cell monolayers were then scratched with a 100 μl pipette tip and washed off the floating cells. Photographs were taken using a phase contrast microscope (AMEX-1200, AMG, Bothell, WA) (×100), and Image J was used to calculate the area of the wound gap.

Transwell invasion assay

Transwell invasion assays were performed using 24-well plates and a transwell invasion chamber (BD Biosciences, SanDiego, CA) with diluted matrix gel (356234, Corning, NY). Then, 5×10^4 cells in 200 μL serum-free medium were inoculated into the upper chamber, and 800 μL medium containing 10% FBS was added to the lower chamber. After incubation for 12 h, the cells were fixed with 4% paraformaldehyde. The matrix gel and the cells at the top of the chamber were scraped with cotton swabs and penetrated cells stained with crystal violet solution (V5265, Sigma-Aldrich). The cells were counted under 5 random visible light microscopes.

Comet assay

After the different treatments of the cells, the DNA damage level was analyzed using a comet assay kit (C2041M, Beyotime, Shanghai, China), according to the reagent manufacturer's instructions. Photographs were taken using a confocal microscope (LSM 510 META, Carl Zeiss, Germany).

X-ray ionizing radiation (IR)

The IR experiments on the cells and BALB/C nude mice were carried out using a PXI X-RAD 225 system (Precision X-ray Inc., North Branford, CT) at the indicated dosages.

Quantitative PCR (qPCR)

The total RNA was obtained using an RNA extraction kit (15596026, Thermo Fisher Scientific), according to the manufacturer's instructions, and a reverse transcription kit (K1621, Thermo Fisher Scientific) was used to obtain cDNA. The SYBR Green kit (4309155, Life technologies corporation, Gaithersburg, MD) was used for qPCR analysis using the quantitative instrument ABI 7500 (Foster city, CA). The primers are listed in Table S3.

Western blot and immunoprecipitation (IP)

The cells were lysed in IP buffer (87787, Thermo Fisher Scientific) containing an inhibitor cocktail (4693116001, Roche, Basel, Switzerland) and a phosphatase inhibitor (4906845001, Roche) for 30 min and then centrifuged at 13,000 rpm at 4 ℃ for 15 min. The protein concentration was measured using BCA reagent (AR0197, Boster Biological Technology, Wuhan, China) and then boiled with 5× buffer. The samples were loaded onto SDS-PAGE gel and transferred to a polyvinylidene fluoride (PVDF) membrane (Merck Millipore, Billerica, MA). The PVDF membrane was incubated overnight with the corresponding primary antibody at 4 ℃ and then incubated with a second antibody at room temperature for 1 h. Finally, the bands were observed using an enhanced chemiluminescence detection kit (36208-A, Yeasen, Shanghai, China).

For the IP experiment, the cell lysate was pre-cleared by incubating with Dynabeads™ protein G (10004d, Invitrogen, Carlsbad, CA). After incubating with the IgG antibody (#2729, Cell Signaling Technology, Danvers, MA) or acetyl lysine antibody (ab21623, Abcam, Cambridge, MA) at 4 ℃ overnight, magnetic beads were added to enrich the acetylated protein for Western blotting analysis.

The antibodies used were as follows: GADD45A (DF6622), p-P38 (AF4001), and p-JNK (AF3318) were purchased from Affinity Biosciences (Cincinnati, OH). NF2 (21686-1-AP), FOXO1 (18592-1-AP), p-AKT (66444-1-Ig), STAT3(10253-2-AP), JNK (66210-1-Ig), AKT (60203-2-Ig), and P38 (66234-1-Ig) were purchased from Proteintech (Chicago, IL). Acetylated histone H4 (GTX122653-S) was purchased from GENETEX (San Antonio, ST). β-actin (AC026) was purchased from ABclonal (Wuhan, China). Acetylated histone H3 (# 8173), p-STAT3 (# 9145), γ-H2AX (# 2577), anti-rabbit IgG-HRP (# 14708), and anti-mouse IgG-HRP (# 14709) were obtained from Cell Signaling Technology.

Dual luciferase reporter assay

The pRL-TK internal control vector and pGL3-Basic-vector or pGL3-basic-GADD45A-promoter plasmids were transfected into the cells. Luciferase activity was detected using a dual-luciferase reporter gene assay kit (RG027, Beyotime), according to the manufacturer's protocol. The

relative luciferase activity was analyzed after normalization against quantified pRL-TK activity.

Animal experiment

Animal experiments were conducted according to the guidelines approved by the Animal Ethics Committee of Medical Research of Central South University. A total of 1×10^7 LN229 cells were subcutaneously injected into 5-week-old female nude mice (BALB/C). The mice were randomly divided into 4 groups (DMSO, PXD101, DMSO + IR, PXD101+IR), with 6 mice in each group. When the tumor volume reached about 50–80 mm^3, PXD101 (50 mg/kg/day) was injected intraperitoneally for 7 consecutive days, and the IR group was treated with 6 Gy after the first injection. The tumor volume was measured every 3 days and was calculated as volume (mm^3)=$d^2\times D/2$, where d and D were the shortest and longest diameters, respectively. At the indicated time points, the mice were sacrificed, and the tumor tissues were weighed, then fixed with 10% buffered formalin for immunohistochemistry (IHC) analysis. For the glioma orthotopic tumor model, the LN229-luc cells were collected, resuspended at 5×10^5 cells in 5 µl of serum-free medium per animal, and then stereotactically injected into the striatum of nude mice. A total of 20 mice were used for the intracranial xenograft tumor model, with 5 mice per group. The tumor cells were implanted into the brains of the nude mice; 14 days later, PXD101 (50 mg/kg/day) was injected intraperitoneally for 7 consecutive days, and the IR group was treated with 6 Gy after the first injection. Tumor growth was measured 30 days after tumor inoculation using an IVIS Lumina III in vivo imaging system (Perkin-Elmer, Waltham, MA, USA).

IHC analysis

Tissue sections of animal tumor samples and 56 paraffin-embedded tumor tissue sections from glioma patients from the Department of Pathology of Xiangya Hospital (2019–2021) were collected [19]. IHC analysis was performed using a universal two-step detection kit (PV-9000, ZSGB-Bio, Beijing, China), according to the manufacturer's instructions; then, the sections were stained with DAB (ZLI-9017, ZSGB-Bio) and counterstained with hematoxylin (E607317, Sangon bio. Shanghai, China). The IHC score was calculated as the product of the intensity value (score 0 to 3) and the positive ratio value (score 0 to 4), as described in the literature [20].

Statistical analysis

Statistical analysis was performed using the GraphPad statistical software program (GraphPad Prism 9, SanDiego, California). The data are expressed as mean ± SD. Differences between groups were assessed using the Student's t-test, and a p-value < 0.05 was considered statistically significant.

Results

PXD101 inhibits proliferation and invasion while promoting apoptosis and radiosensitivity in GBM cells

To investigate the role of PXD101 in GBM cells, an MTS assay was performed, and the data showed that PXD101 inhibited the GBM cell proliferation in a concentration- and time-dependent manner. After 48 h of PXD101 treatment, the IC_{50} of the T98G cells was approximately 5 µM, and the IC_{50} of the LN229 cells was approximately 1 µM (Fig. 1A). Additionally, the colony formation assay results demonstrated that PXD101 inhibited the proliferation of GBM cells (Fig. 1B). The flow cytometry analysis revealed that PXD101 induced cell apoptosis (Fig. 1C). The scratch and transwell assays indicated that PXD101 could significantly inhibit the migration and invasion of GBM cells (Fig. 1D, E). Moreover, the results of the radiosensitivity analysis showed that the cell survival fraction of the PXD101-treated group was significantly lower than that of the control group under IR treatment (Fig. 1F). The comet assay and Western blot experiments results showed that PXD101 could improve the DNA damage level and upregulate the protein expression of γ-H2AX in the GBM cells, especially under IR treatment (Fig. 1G, H). These results indicate that PXD101 could effectively inhibit the malignant progression and radioresistance of GBM cells.

PXD101 induces the expression of GADD45A

In malignant tumors, tumor suppressor genes are often silenced through deacetylation; so, HDACi can promote the expression of tumor suppressor genes through restoring acetylation [21]. Therefore, through literature review, 55 genes related to GBM and involved in radioresistance of malignant tumors were selected from 1018 protein coding genes in the TSGene2.0 tumor suppressor gene library [22], for qPCR array screening after PXD101 treatment (Fig. 2A). The results showed that there were 13 genes with significant upregulation (fold change > 4), including DKK1, MXI1, GADD45B, NF2, DAPK3, ING1, TNF10A, FOXO6, PTEN, GADD45A, RASSF4, TP63, and FOXO1. We then used qPCR to detect the expression of the 13 increased genes. The results showed that the mRNA expression levels of GADD45A, NF2, and FOXO1 were most significantly increased in both of the GBM cell lines, T98G and LN229 ($P<0.001$) (Fig. 2B). Furthermore, the Western blot data showed that GADD45A protein expression was significantly enhanced after PXD101 treatment, while the protein expression of NF2 and FOXO1 did not significantly change in the three GBM cell lines (Fig. 2C). Furthermore, we found that the protein expression of GADD45A was most significantly

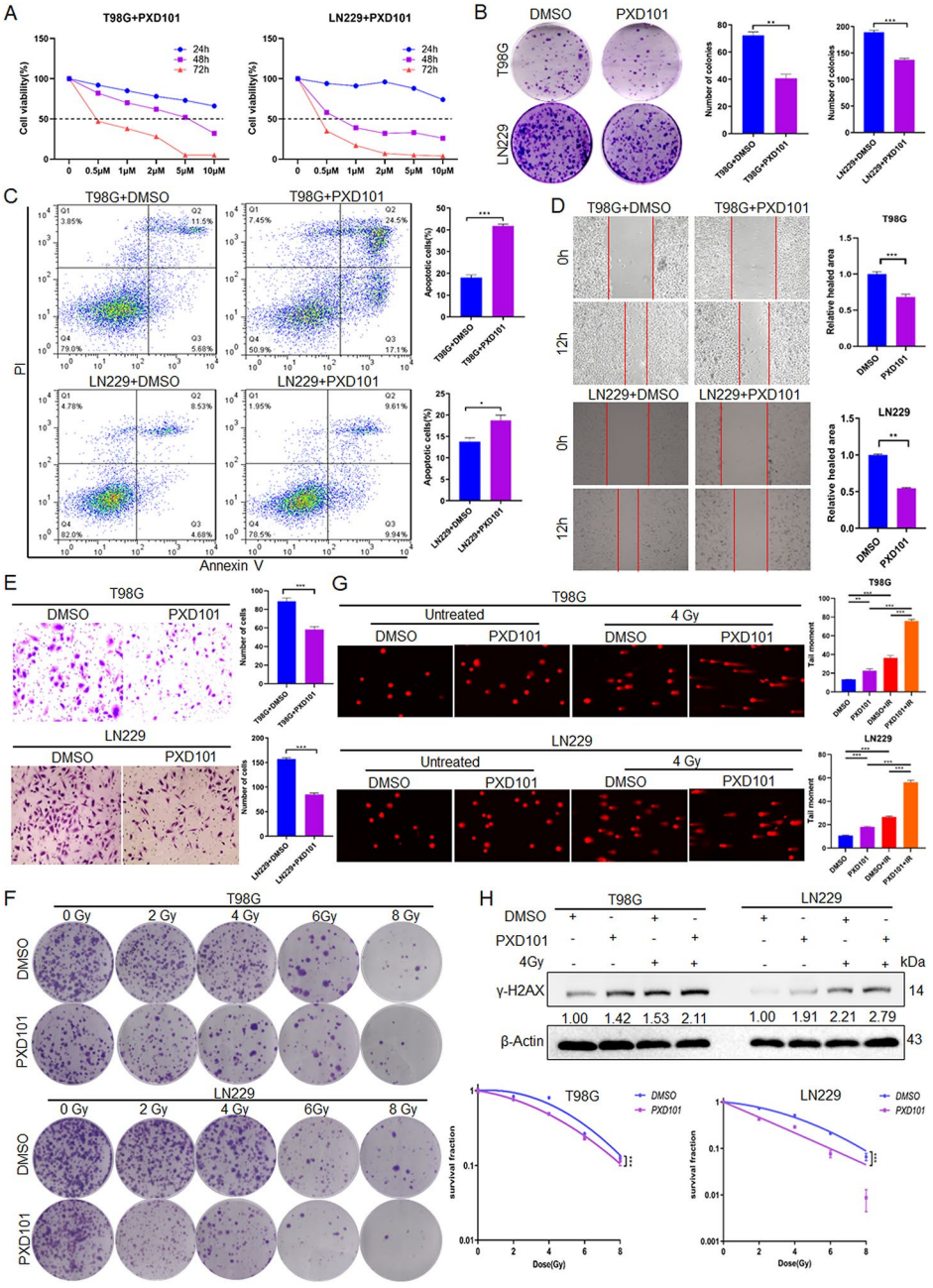

Fig. 1 PXD101 inhibits proliferation and invasion while promoting apoptosis and radiosensitivity in GBM cells. (**A**) T98G and LN229 cells were treated with different concentrations of PXD101 (0, 0.5, 2, 5, 10μM), and the cell viability was detected using an MTS assay. T98G cells and LN229 cells were treated with PXD101 (5μM, 1μM), respectively. (**B**) Clone formation assay was used to detect the cell proliferation. (**C**) Flow cytometry was used to analyze the cell apoptosis. (**D**) Scratch assay was used to detect the cell migration. (**E**) Transwell assay was used to analyze the cell invasion ability. (**F**) The cell survival fraction was detected using radiosensitivity analysis after 12 h of different IR doses (0 Gy, 2 Gy, 4 Gy, 6 Gy, 8 Gy) treatment. T98G cells and LN229 cells were treated with PXD101 (5μM, 1μM); then, the cells were treated with 4 Gy radiation; (**G**) The comet assay was used to analyze the DNA damage. (**H**) The protein expression of γ-H2AX was analyzed using Western blot. Data are shown as the mean ± SD of three independent experiments. $^{*}P < 0.05$, $^{**}P < 0.01$, $^{***}P < 0.001$

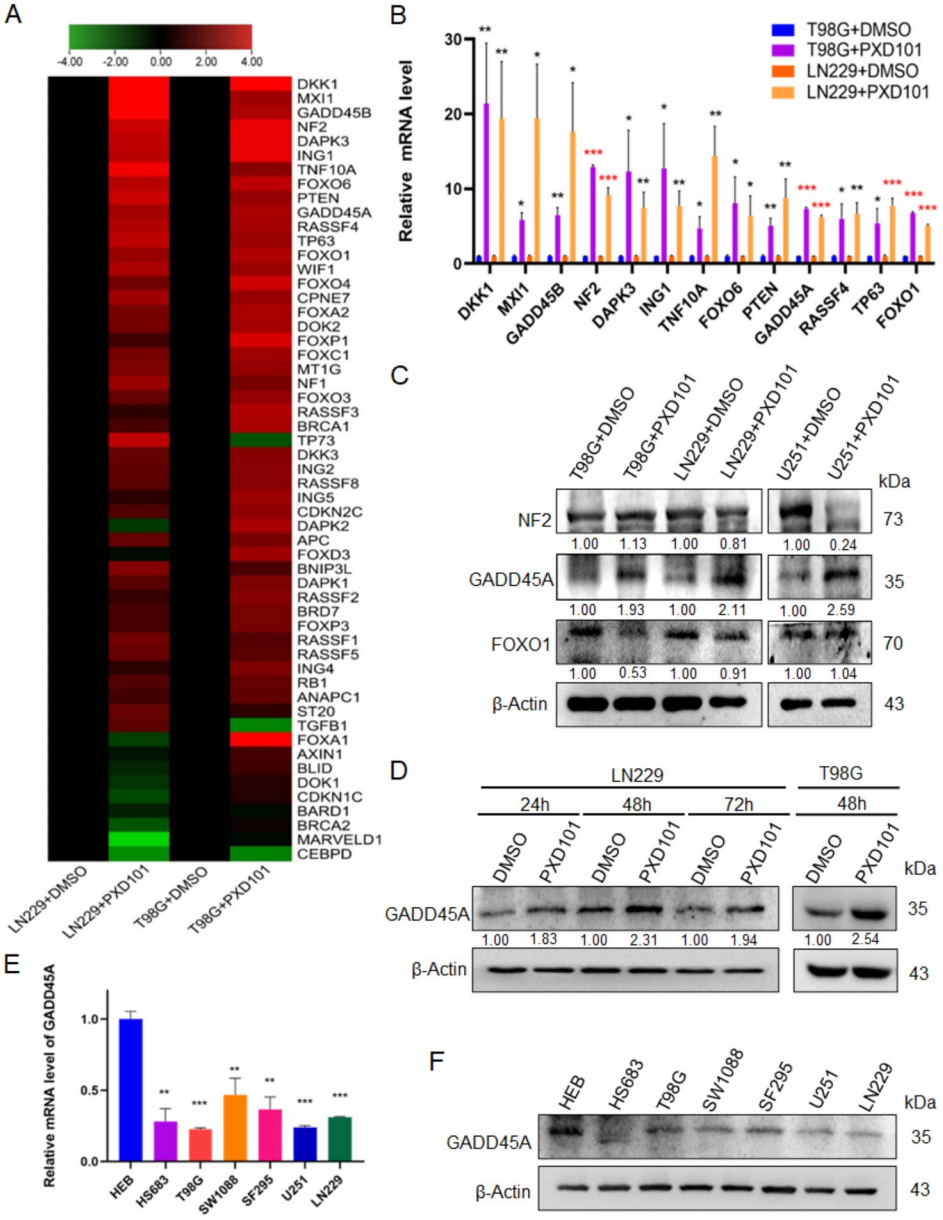

Fig. 2 PXD101 induces the expression of GADD45A. T98G cells and LN229 cells were treated with PXD101 (5μM, 1μM) for 24 h, respectively. (**A**) qPCR array analyses of 55 tumor suppressor genes in GBM cells are displayed using a heatmap. (**B**) The mRNA expressions of DKK1, MXI1, GADD45B, NF2, DAPK3, ING1, TNF10A, FOXO6, PTEN, GADD45A, RASSF4, TP63, and FOXO1 were detected using qPCR. (**C**) The protein expressions of NF2, GADD45A, and FOXO1 were analyzed using Western blot. (**D**) LN229 cells were treated with PXD101 (1μM) for 24 h, 48 h, and 72 h, respectively, and T98G cells were treated with PXD101 (5μM) for 48 h. The GADD45A expression was detected using Western blot. (**E**-**F**) The mRNA and protein expressions of GADD45A were detected using qPCR (**E**) and Western blot (**F**) in the normal glial cells HEB and glioma cells. Data are shown as the mean ± SD of three independent experiments. *$P < 0.5$, **$P < 0.01$, ***$P < 0.001$

increased after PXD101 treatment for 48 h (Fig. 2D). These results suggest that PXD101 can upregulate the mRNA and protein expression of GADD45A in GBM cells. Moreover, compared with the normal glial cell line HEB, the mRNA and protein expressions of GADD45A were decreased (Fig. 2E, F). These results indicate that GADD45A could be a key suppressor molecule in the role of PXD101 in GBM.

PXD101 inhibits malignant progression and radioresistance of GBM cells through GADD45A

To determine whether PXD101 exerts its antitumor function in GBM cells through GADD45A, the T98G and LN229 cells were treated with PXD101 and GADD45A knockdown, while the U251 cells were treated with PXD101 and GADD45A overexpression (Fig. 3A). The results of the MTS assay showed that the cell proliferation was significantly inhibited in the PXD101 treatment

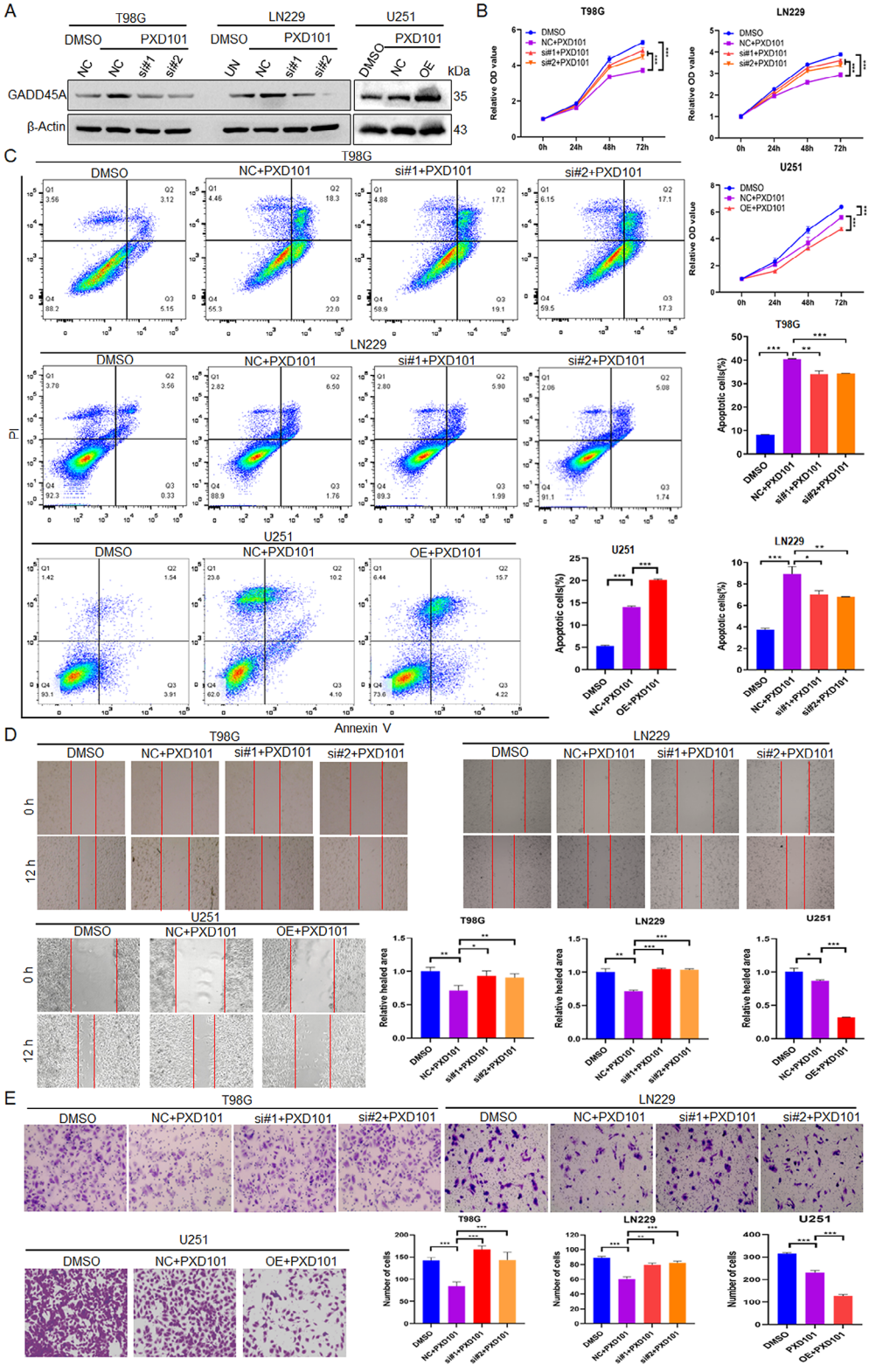

Fig. 3 PXD101 inhibits malignant progression of GBM cells through GADD45A. T98G cells and LN229 cells were treated with PXD101 (5μM, 1μM) and transfected with GADD45A siRNA; U251 cells were treated with PXD101 (1μM) and transfected with GADD45A-OE plasmid. (**A**) The GADD45A expression was detected using Western blot. (**B**) MTS assay was used to detect the cell proliferation. (**C**) Flow cytometry was used to analyze the apoptosis. (**D**) Scratch assay was used to detect cell migration ability. (**E**) Transwell assay was used to analyze cell invasion. Data are shown as the mean ± SD of three independent experiments. NC: negative control. *$P < 0.5$, **$P < 0.01$, ***$P < 0.001$

group. Furthermore, knocking down GADD45A could restore most of the inhibition, and overexpressed GADD45A could enhance the inhibition (Fig. 3B). Similarly, the flow cytometry data showed that GADD45A knockdown could reduce the PXD101-mediated apoptosis of GBM cells to a large extent, while GADD45A overexpression had the opposite effect (Fig. 3C). The results of the scratch and transwell assays also showed that GADD45A knockdown could effectively restore the PXD101-mediated reduction in cell migration and invasion and that overexpressed GADD45A could enhance PXD101-mediated inhibition (Fig. 3D, E). Importantly, the results of the radiosensitivity analysis revealed that PXD101 promoted the radiosensitivity of GBM cells, while further knocking down GADD45A reversed this effect (Fig. 4A). Consistent with this, the comet assay and Western blot results showed that GADD45A knockdown could reverse the PXD101-mediated DNA damage (Fig. 4B) and γ-H2AX expression (Fig. 4C). These results indicate that PXD101 exerts its antitumor effect in GBM cells through GADD45A .

PXD101 upregulates GADD45A expression through histone acetylation to mediate the activation of P38

Research has shown that HDACi can not only directly deacetylate target proteins to alter their structure and function but also change the expression of target proteins by regulating histone acetylation [23]. To investigate the upregulating mechanism of GADD45A utilized by PXD101, the IP experiment was performed using the acetyl lysine antibody. The results showed that the direct acetylation of GADD45A did not occur under the PXD101 treatment (Fig. 5A). However, the acetylation levels of histone H3 and histone H4 were significantly upregulated (Fig. 5B); this indicates that PXD101 could upregulate GADD45A by promoting histone acetylation. Furthermore, the results of the dual-luciferase reporter gene showed that PXD101 significantly increased the transcriptional activity of GADD45A (Fig. 5C). Studies have shown that GADD45A can participate in the regulation of the AKT, JNK, P38, and STAT3 pathways [24]. After the overexpression of GADD45A (Fig. 5D), the Western blot results showed that the phosphorylation of P38 (Thr180/Tyr182) was significantly increased, while the phosphorylation of AKT (Ser473), JNK (Thr183/Tyr185), and STAT3 (Tyr705) did not change significantly (Fig. 5E). Further experiments showed that the expression of GADD45A was upregulated after PXD101 treatment and that the phosphorylation level of P38 was significantly upregulated (Fig. 5F). These results indicate that PXD101 can promote P38 phosphorylation activation by inducing GADD45A expression through histone acetylation.

PXD101 inhibits the growth and radioresistance of GBM in vivo

To evaluate the effect of PXD101 on the growth and radiotherapy of glioma in vivo, the LN229 cells were used to establish a GBM xenograft model in the nude mice, and the PXD101, IR, and combination treatments were used, respectively. The results showed that compared with the DMSO control group, both the PXD101 and IR treatments inhibited tumor growth, while PXD101 combined with IR inhibited tumor growth more significantly (Fig. 6A-C). Meanwhile, PXD101 had no significant effect on the body weights of the mice (Fig. 6D). IHC analysis revealed that compared with the DMSO and IR treatments, the expression of GADD45A and p-P38 in the tumor tissues was significantly upregulated after the PXD101 or combination treatments (Fig. 6E). Given that PXD101 is a drug that can cross the blood–brain barrier, we further explored the effect of PXD101 on radiotherapy sensitization in a mouse orthotopic tumor (Fig. 6F). The results showed that compared with the DMSO control group, both the PXD101 and IR treatments inhibited tumor growth (Fig. 6G) and improved the survival rate of the tumor-bearing mice, and the combined treatment had a more significant inhibitory effect (Fig. 6H). Similarly, PXD101 had no significant effect on the body weights of the mice (Fig. 6I). In addition, IHC analysis of 56 GBM clinical samples also found that p-P38 expression was lower in the GADD45A low-expression group, and correlation analysis showed that there was a positive correlation between GADD45A and p-P38 (Fig. 6J). These results suggest that PXD101 could inhibit the growth and radioresistance of GBM in vivo.

Discussion

A few studies have shown that HDACi combined with radiotherapy is effective for GBM. HDACi valproic acid (VPA) could sensitize GBM cells to radiation [25]. HDACi SAHA had a radiosensitizing effect in GBM cells through the modulation of DNA damage response [26]. In this study, we found that the radiosensitivity of the GBM cells was improved using the combination of the PXD101 and IR treatments. In the in vivo experiment, the tumor growth was weakened when treated with PXD101 and was more significantly inhibited when this treatment was combined with the IR treatment. Therefore, our study showed that PXD101, as an HDACi that can penetrate the blood–brain barrier effectively, may be a new radiosensitizer for GBM radiotherapy.

A common feature of malignant tumors is the overall low acetylation of histone H3/H4 [27], and the loss of histone acetylation is an early event of tumor suppressor gene silencing [28]. In our study, we also found that the levels of histone H3/H4 acetylation were significantly enhanced in the PXD101-treated GBM cells.

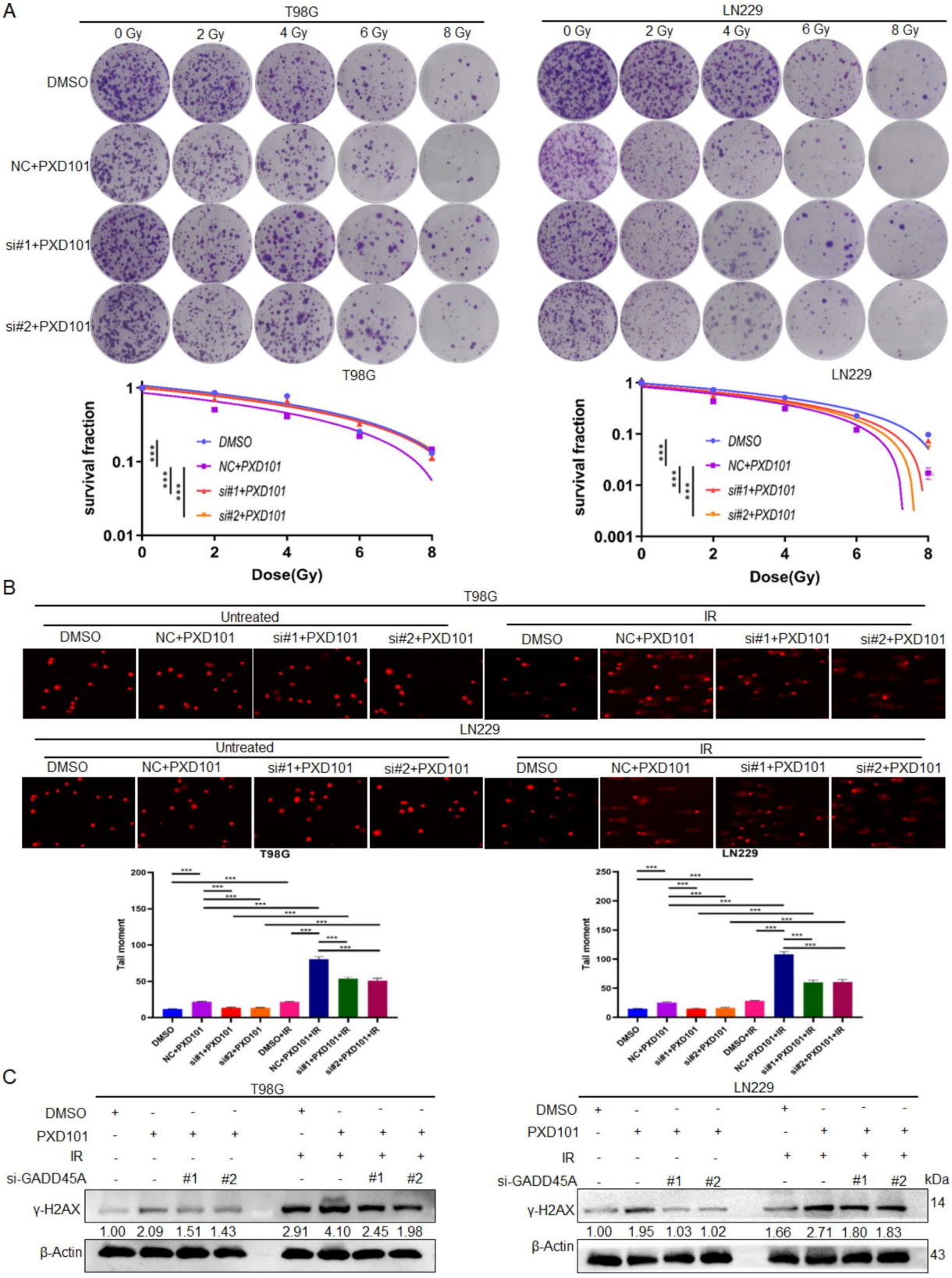

Fig. 4 PXD101 inhibits radioresistance of GBM cells through GADD45A. T98G cells and LN229 cells were treated with PXD101 (5μM, 1μM) and transfected with GADD45A siRNA. (**A**) The survival fractions of T98G cells and LN229 cells were detected using radiosensitivity analysis after 12 h of different IR doses (0 Gy, 2 Gy, 4 Gy, 6 Gy, 8 Gy) treatment. (**B**) Comet assay was used to analyze the DNA damage. (**C**) The protein expression of γ-H2AX was analyzed using Western blot. Data are shown as the mean ± SD of three independent experiments. NC: negative control. ***$P < 0.001$

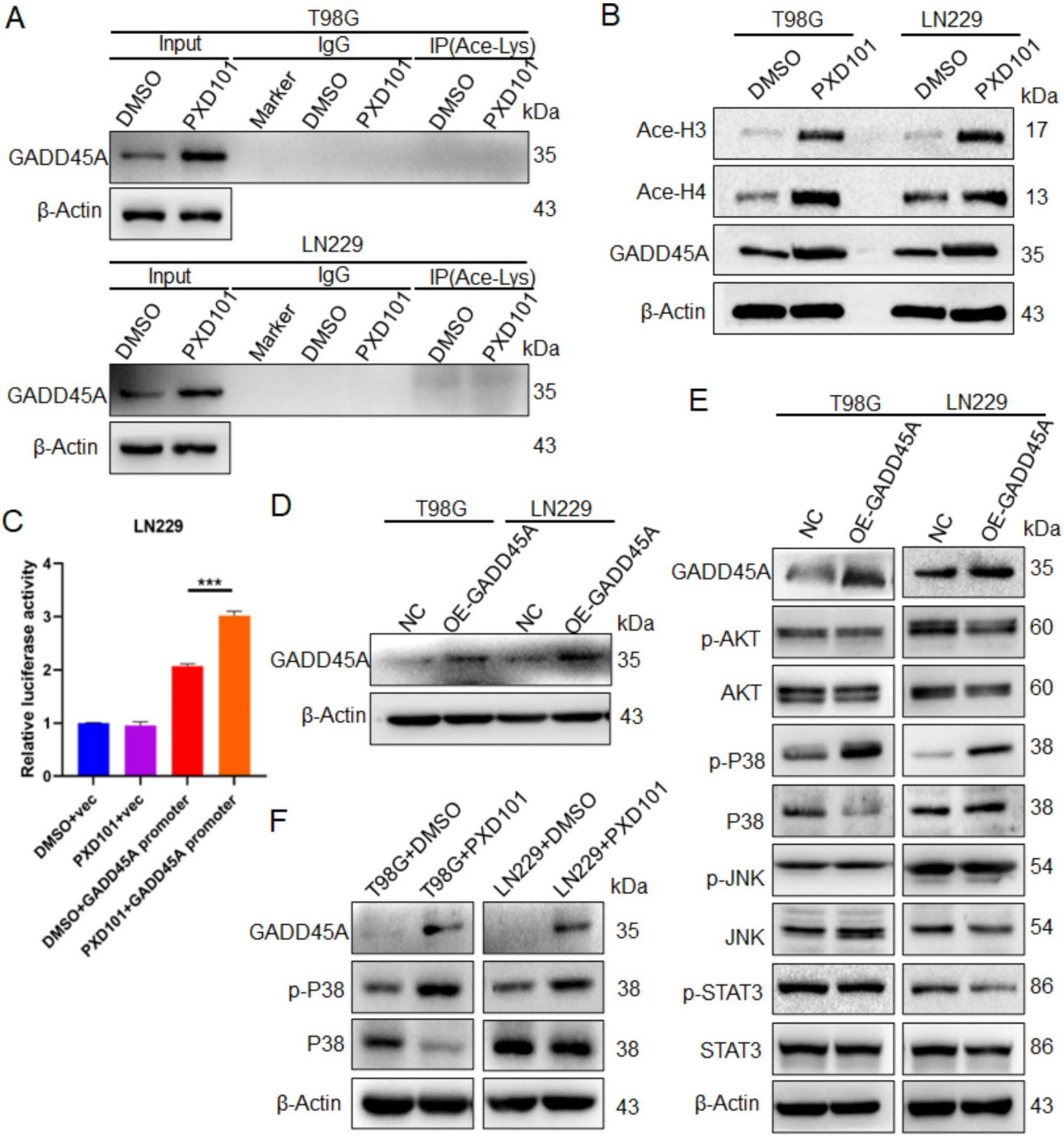

Fig. 5 PXD101 upregulates GADD45A expression through histone acetylation to mediate the activation of P38. T98G cells and LN229 cells were treated with PXD101 (5μM, 1μM), respectively. (**A**) The acetylation level of GADD45A was detected using IP assay with acetyl lysine antibody. (**B**) The protein expression of acetylated histone H3, H4, and GADD45A was detected using Western blot. T98G cells and LN229 cells were transfected with GADD45A-OE plasmid. (**C**) LN229 cells were transfected with pGL3-basic-GADD45A-promoter or pGL3-basic-vector plasmids. Subsequently, cells were treated with DMSO or PXD101 (1μM); then, the transcriptional activity of GADD45A was detected using dual-luciferase assay. (**D**) The GADD45A expression was detected using Western blot. (**E**) The protein expressions of GADD45A, AKT, p-AKT, P38, p-P38, JNK, p-JNK, STAT3, and p-STAT3 were analyzed using Western blot. (**F**) T98G cells and LN229 cells were treated with PXD101 (5μM, 1μM), respectively; the protein expressions of GADD4A, P38, and p-P38 were detected using Western blot. NC: negative control

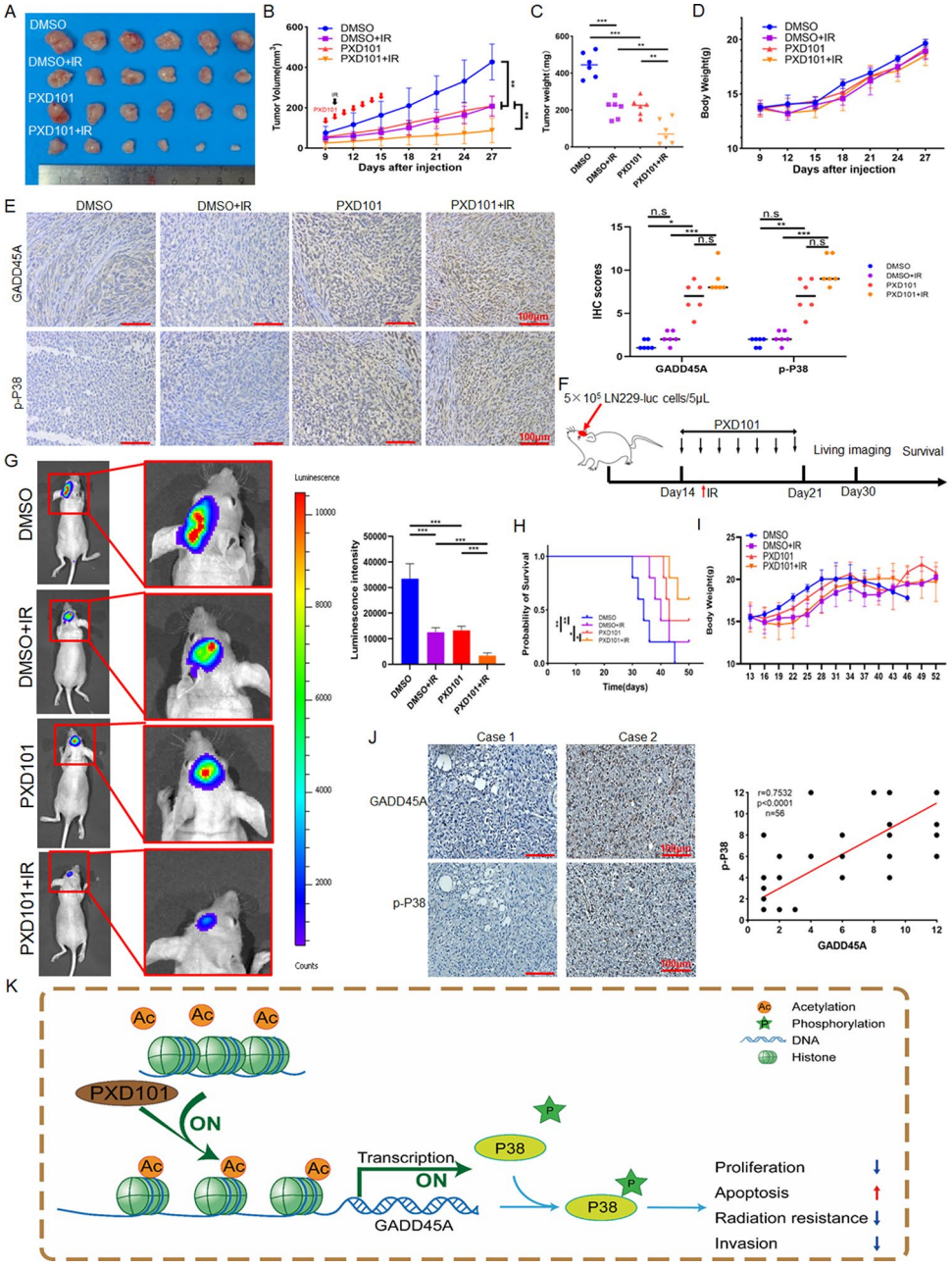

Fig. 6 PXD101 inhibits the growth and radioresistance of GBM in vivo. A total of 1×10^7 LN229 cells were inoculated into the armpits of nude mice, and the PXD101 treatment group was injected intraperitoneally with PXD101 (50 mg/kg) for 7 days; the IR group was irradiated with 6 Gy after the first injection. (**A**-**D**): Tumor size (**A**), tumor volume (**B**), tumor weight (**C**), and body weight (**D**) were measured. (**E**) The representative images of IHC staining of GADD45A and p-P38 in xenograft tumor tissues (left). The statistical analysis of IHC score (right). (**F**) Schematic diagram of the orthotopic tumor mouse model. (**G**) Representative bioluminescence images of PXD101 or/and IR treatment after intracranial injection of LN229-luc cells in mice ($n = 5$) (left); quantitative analysis of the bioluminescence intensity (right). (**H**) Kaplan–Meier survival curves of mice. (**I**) The curves of mice body weight. (**J**) The representative images of IHC staining of GADD45A and p-P38 protein levels in clinical samples (left); the correlation analysis of GADD45A and p-P38 expression based on IHC score (right). (**K**) Schematic diagram of PXD101 inhibiting malignant progression and radioresistance of GBM by promoting GADD45A/p-P38 pathway. Scale bar, 100 μm. *$P < 0.5$, **$P < 0.01$, ***$P < 0.001$

Recent studies have found that HDACi directly acetylated the target protein. By inhibiting the deacetylase HDAC4, tasquinimod promoted the acetylation of phosphatase LHPP and protein stability and inhibited nasopharyngeal carcinoma proliferation and metastasis [29]. HDAC3-IN-T247 and T326 increased the acetylation of NF-κB by inhibiting the activity of HDAC3, thereby inhibiting the growth of colorectal cancer cells [30]. We did not find direct protein acetylation of GADD45A in the GBM cells after the treatment with PXD101;

however, we did find upregulated GADD45A transcription through the increasing of the histone acetylation.

GADD45A has been reported to regulate numerous cellular processes associated with stress signaling and injury response [31]. Studies have shown that GADD45A expression is often downregulated in various tumors, such as cervical cancer, breast cancer, colorectal cancer, and bladder cancer [24]. At present, GADD45A mainly plays an antitumor role and promotes radiosensitivity in tumor cells. The overexpression of GADD45A could enhance the radiosensitivity of human tongue squamous cell carcinoma cells [32]. GADD45A could reduce the distribution of cytoplasmic APE1, thereby enhancing the radiosensitivity of cervical cancer cells [33]. In medulloblastoma, GADD45A had an antitumor effect and sensitized cells to radiotherapy through the negative regulation of matrix metallopeptidase (MMP)-9 and β-catenin [34]. These results showed that the overexpression of GADD45A significantly enhanced radiosensitivity, probably via its roles in the control of the cell cycle, cell death, and DNA repair. Despite its well-established tumor suppressor properties, GADD45A also has antiapoptotic and pro-survival effects in some malignancies, and there is evidence that its gene expression is positively correlated with the development of some tumors [35]. In prostate cancer, the inhibition of GADD45A activity made the tumor cells more sensitive to IR [36]. In the present study, the results indicated that PXD101 can enhance the radiosensitivity of GBM by upregulating GADD45A.

In tumor cells, GADD45A can regulate multiple signaling pathways. GADD45A enhanced chemosensitivity to oxaliplatin in hepatocellular carcinoma cells by inhibiting the PI3K/AKT signaling pathway [37]. GADD45A inhibited the progression of Ras-driven breast cancer through the JNK signaling pathway [38]. GADD45A could bind to mTOR and inhibit tumor angiogenesis by inhibiting the activation of STAT3 and VEGFα in embryonic fibroblasts [39]. GADD45A could activate the P38/mitogen-activated protein kinase (MAPK) signaling pathway and inhibit the activity of the trophoblast cells [40]. However, in this study, most of the above signaling pathways were not validated after overexpression of GADD45A in the GBM cells, and we found that the phosphorylation level of P38 was significantly increased. It may be mediated by these different protein interactions and may depend on the biological environment, including cell type, developmental stage, and stress/stimulation. The P38 pathway mainly plays a pro-tumor function in tumors, such as in colorectal cancer, where P38 mediates the stability of FOXC1 protein and promoted tumor metastasis [41]. In bladder cancer, P38 regulates the expression of several MMPs, promoting tumor migration and invasion [42]. In breast cancer, P38 modulates the expression of pro-angiogenic factors, such as HBEGF, IL-8, and VEGFA, to enhance tumor vascularization and metastasis [43]. Conversely, the P38 pathway also has an inhibitory effect on cancer. In a breast cancer stem cell model, the activation of the P38 and AMPKα pathways could induce G0/G1 arrest and intrinsic apoptosis, thereby inhibiting tumor growth [44]. In metastatic prostate cancer cells, the activation of P38 is induced by TGFβRII, which phosphorylates RB to prevent bone metastasis [45]. In our study, the animal experiment results further confirmed that PXD101 could inhibit the tumor growth of GBM, inducing the expression of GADD45A and activating the P38 signal.

Despite PXD101 being approved for the treatment of hematologic malignancies, therapeutic outcomes in solid tumors have so far been limited. This is likely due to its shortened half-life and underlying pharmacokinetics [46]; it has been reported that a novel PXD101 prodrug or drug delivery system was designed to overcome the pharmacokinetic challenges [47, 48]. Meanwhile, PXD101 has shown little activity as a single agent in solid tumor trials; it has been reported that the combination of PXD101 with cisplatin and etoposide was safe and active in lung cancer patients [49]. PXD101 has been shown to have the potential to enhance chemoradiation in GBM [50]; thus, further in vivo studies will provide more information about the anti-GBM effectiveness of PXD101, while considering its metabolic dynamics and efficiency in crossing the blood–brain barrier.

In summary, PXD101 could inhibit GBM proliferation, invasion, and radioresistance by upregulating GADD45A. Mechanically, PXD101 promoted the transcription of GADD45A by directly acetylating histones H3/H4 and further activating the P38 signal pathway. This finding elucidates the molecular mechanism of PXD101 as a treatment for GBM and provides a theoretical basis for the radiosensitization of GBM (Fig. 6K).

Abbreviations

GBM	Glioblastoma
TMZ	Temozolomide
HDAC	Histone Deacetylase
HAT	Histone acetyltransferase
HDACi	Histone Deacetylase Inhibitor
GADD45A	Growth Arrest and DNA Damage-Inducible Protein a
PI	Propidium Iodide
IR	X-ray Ionizing Radiation
qPCR	Quantitative PCR
IP	Immunoprecipitation
PVDF	Polyvinylidene Fluoride
IHC	Immunohistochemistry
VPA	Valproic Acid
MMP	matrix metallopeptidase
MAPK	Mitogen-Activated Protein Kinase

Supplementary Information

The online version contains supplementary material available at https://doi.org/10.1186/s12967-024-05874-5.

Supplementary Material 1

Acknowledgements
Not applicable.

Author contributions
XHH: Data curation, visualization, formal analysis, investigation. PJZ: Data curation, investigation, validation, writing–original draft. XZP: Data curation, software. YTOY: Investigation, methodology. DL: Resources, supervision. XW: Conceptualization, formal analysis, investigation, methodology, writing–review and editing. LFY: Conceptualization, data curation, formal analysis, supervision, funding acquisition, investigation, methodology, writing–review and editing. All authors read and approved the final manuscript.

Funding
This work was supported by the grants from the National Nature Science Foundation of China (No: 82103471), the Natural Science Foundation of Hunan Province, China (No: 2022JJ30059), and the Fundamental Research Funds for the Central Universities of Central South University (No: 2024ZZTS0912).

Data availability
All data generated or analyzed during this study are included in this published article and its supplementary information files.

Declarations

Ethics approval and consent to participate
This study was performed in line with the principles of the Declaration of Helsinki. Approval was granted by the Animal Ethics Committee of Medical Research of Central South University (Changsha, China).

Consent for publication
Informed consent was obtained from all individual participants included in the study.

Competing interests
The authors declare that they have no competing interests.

Received: 3 July 2024 / Accepted: 11 November 2024
Published online: 20 November 2024

References

1. Louis DN, Perry A, Wesseling P, Brat DJ, Cree IA, Figarella-Branger D, Hawkins C, Ng HK, Pfister SM, Reifenberger G, Soffietti R, von Deimling A, Ellison DW. The 2021 WHO classification of tumors of the central nervous system: a summary. Neuro Oncol. 2021;23(8):1231–51.
2. Hombach-Klonisch S, Mehrpour M, Shojaei S, Harlos C, Pitz M, Hamai A, et al. Glioblastoma and chemoresistance to alkylating agents: involvement of apoptosis, autophagy, and unfolded protein response. Pharmacol Ther. 2018;184:13–41.
3. Rong L, Li N, Zhang Z. Emerging therapies for glioblastoma: current state and future directions. J Exp Clin Cancer Res. 2022;41(1):142.
4. Louis DN, Perry A, Reifenberger G, von Deimling A, Figarella-Branger D, Cavenee WK, et al. The 2016 World Health Organization Classification of Tumors of the Central Nervous System: a summary. Acta Neuropathol. 2016;131:803–20.
5. Saha RN, Pahan K. HATs and HDACs in neurodegeneration: a tale of disconcerted acetylation homeostasis. Cell Death Differ. 2006;13:539–50.
6. Mottet D, Pirotte S, Lamour V, Hagedorn M, Javerzat S, Bikfalvi A, et al. HDAC4 represses p21(WAF1/Cip1) expression in human cancer cells through a Sp1-dependent, p53-independent mechanism. Oncogene. 2009;28:243–56.
7. Funato K, Hayashi T, Echizen K, Negishi L, Shimizu N, et al. SIRT2-mediated inactivation of p73 is required for glioblastoma tumorigenicity. EMBO Rep. 2018;19(11):e45587.
8. Lane AA, Chabner BA. Histone deacetylase inhibitors in cancer therapy. J Clin Oncology: Official J Am Soc Clin Oncol. 2009;27:5459–68.
9. Chang HH, Chang YY, Tsai BC, Chen LJ, Chang AC, Chuang JY, Gean PW, Hsueh YS. A selective histone deacetylase inhibitor induces autophagy and cell death via SCNN1A downregulation in Glioblastoma Cells. Cancers (Basel). 2022;14(18):4537.
10. Jin H, Liang L, Liu L, Deng W, Liu J. HDAC inhibitor DWP0016 activates p53 transcription and acetylation to inhibit cell growth in U251 glioblastoma cells. J Cell Biochem. 2013;114(7):1498–509.
11. Kuribayashi T, Ohara M, Sora S, Kubota N. Scriptaid, a novel histone deacetylase inhibitor, enhances the response of human tumor cells to radiation. Int J Mol Med. 2010;25(1):25–9.
12. Folkvord S, Ree Ah Fau - Furre T, Furre T, Fau - Halvorsen T, Halvorsen T, Fau - Flatmark K, Flatmark K. Radiosensitization by SAHA in experimental colorectal carcinoma models-in vivo effects and relevance of histone acetylation status. Int J Radiat Oncol Biol Phys. 2009;74(2):546–52.
13. Pojani E, Barlocco D. Romidepsin (FK228), a histone deacetylase inhibitor and its Analogues in Cancer Chemotherapy. Curr Med Chem. 2021;28:1290–303.
14. El Omari N, Bakrim S, Khalid A, Albratty M, Abdalla AN, Lee LH, Goh KW, Ming LC, Bouyahya A. Anticancer clinical efficiency and stochastic mechanisms of belinostat. Biomed Pharmacother. 2023;165:115212.
15. Chan D, Zheng Y, Tyner JW, Chng WJ, Chien WW, Gery S, Leong G, Braunstein GD, Koeffler HP. Belinostat and panobinostat (HDACI): in vitro and in vivo studies in thyroid cancer. J Cancer Res Clin Oncol. 2013;139(9):1507–14.
16. Wang B, Wang XB, Chen LY, Huang L, Dong RZ. Belinostat-induced apoptosis and growth inhibition in pancreatic cancer cells involve activation of TAK1-AMPK signaling axis. Biochem Biophys Res Commun. 2013;437(1):1–6.
17. Marampon F, Di Nisio V, Pietrantoni I, Petragnano F, Fasciani I, Scicchitano BM, et al. Pro-differentiating and radiosensitizing effects of inhibiting HDACs by PXD-101 (Belinostat) in in vitro and in vivo models of human rhabdomyosarcoma cell lines. Cancer Lett. 2019;461:90–101.
18. Kusaczuk M, Kretowski R, Stypulkowska A, Cechowska-Pasko M. Molecular and cellular effects of a novel hydroxamate-based HDAC inhibitor - belinostat - in glioblastoma cell lines: a preliminary report. Invest New Drugs. 2016;34:552–64.
19. Zhou P, Peng X, Tang S, Zhang K, Tan Z, Li D, et al. E3 ligase MAEA-mediated ubiquitination and degradation of PHD3 promotes glioblastoma progression. Oncogene. 2023;42:1308–20.
20. Wu X, Zhou Z, Xu S, Liao C, Chen X, Li B, et al. Extracellular vesicle packaged LMP1-activated fibroblasts promote tumor progression via autophagy and stroma-tumor metabolism coupling. Cancer Lett. 2020;478:93–106.
21. Li Y, Seto E. HDACs and HDAC inhibitors in Cancer Development and Therapy. Cold Spring Harb Perspect Med. 2016;6(10):a026831.
22. Zhao M, Kim P, Mitra R, Zhao J, Zhao Z. TSGene 2.0: an updated literature-based knowledgebase for tumor suppressor genes. Nucleic Acids Res. 2016;44:D1023–1031.
23. Eckschlager T, Plch J, Stiborova M, Hrabeta J. Histone deacetylase inhibitors as anticancer drugs. Int J Mol Sci. 2017;18(7):1414.
24. Palomer X, Salvador JM, Grinan-Ferre C, Barroso E, Pallas M, Vazquez-Carrera M. GADD45A: with or without you. Med Res Rev. 2024;44(4):1375–403.
25. Krauze AV, Myrehaug SD, Chang MG, Holdford DJ, Smith S, Shih J, Tofilon PJ, Fine HA, Camphausen K. A phase 2 study of Concurrent Radiation Therapy, Temozolomide, and the histone deacetylase inhibitor valproic acid for patients with Glioblastoma. Int J Radiat Oncol Biol Phys. 2015;92(5):986–92.
26. Barazzuol L, Jeynes JC, Merchant MJ, Wera AC, Barry MA, Kirkby KJ, et al. Radiosensitization of glioblastoma cells using a histone deacetylase inhibitor (SAHA) comparing carbon ions with X-rays. Int J Radiat Biol. 2015;91:90–8.
27. Fraga MF, Ballestar E, Villar-Garea A, Boix-Chornet M, Espada J, Schotta G, et al. Loss of acetylation at Lys16 and trimethylation at Lys20 of histone H4 is a common hallmark of human cancer. Nat Genet. 2005;37:391–400.
28. Mutskov V, Felsenfeld G. Silencing of transgene transcription precedes methylation of promoter DNA and histone H3 lysine 9. EMBO J. 2004;23:138–49.
29. Sun X, Zhang K, Peng X, Zhou P, Qu C, Yang L, et al. HDAC4 mediated LHPP deacetylation enhances its destabilization and promotes the proliferation and metastasis of nasopharyngeal carcinoma. Cancer Lett. 2023;562:216158.
30. Suzuki T, Kasuya Y, Itoh Y, Ota Y, Zhan P, Asamitsu K, et al. Identification of highly selective and potent histone deacetylase 3 inhibitors using click Chemistry-based combinatorial Fragment Assembly. PLoS ONE. 2013;8(7):e68669.
31. Patel K, Murray MG, Whelan KA. Roles for GADD45 in Development and Cancer. Adv Exp Med Biol. 2022;1360:23–39.
32. Zhang XY, Qu X, Wang CQ, Zhou CJ, Liu GX, Wei FC, Sun SZ. Over-expression of Gadd45a enhances radiotherapy efficacy in human Tca8113 cell line. Acta Pharmacol Sin. 2011;32(2):253–8.

33. Li Q, Wei X, Zhou ZW, Wang SN, Jin H, Chen KJ, et al. GADD45α sensitizes cervical cancer cells to radiotherapy via increasing cytoplasmic APE1 level. Cell Death Dis. 2018;9:524.
34. Asuthkar S, Nalla AK, Gondi CS, Dinh DH, Gujrati M, Mohanam S, et al. Gadd45a sensitizes medulloblastoma cells to irradiation and suppresses MMP-9-mediated EMT. Neuro Oncol. 2011;13:1059–73.
35. Tront JS, Huang Y, Fornace AA Jr., Hoffman B, Liebermann DA. Gadd45a functions as a promoter or suppressor of breast cancer dependent on the oncogenic stress. Cancer Res. 2010;70(23):9671–81.
36. Lu X, Yang C, Hill R, Yin C, Hollander MC, Fornace AJ Jr, et al. Inactivation of gadd45a sensitizes epithelial cancer cells to ionizing radiation in vivo resulting in prolonged survival. Cancer Res. 2008;68:3579–83.
37. Wang X, Zou F, Zhong J, Yue L, Wang F, Wei H, et al. Secretory clusterin mediates Oxaliplatin Resistance via the Gadd45a/PI3K/Akt signaling pathway in Hepatocellular Carcinoma. J Cancer. 2018;9:1403–13.
38. Tront JS, Hoffman B, Liebermann DA. Gadd45a suppresses ras-driven mammary tumorigenesis by activation of c-Jun NH2-terminal kinase and p38 stress signaling resulting in apoptosis and senescence. Cancer Res. 2006;66:8448–54.
39. Yang F, Zhang W, Li D, Zhan Q. Gadd45a suppresses tumor angiogenesis via inhibition of the mTOR/STAT3 protein pathway. J Biol Chem. 2013;288:6552–60.
40. Qian X, Zhang Y. EZH2 enhances proliferation and migration of trophoblast cell lines by blocking GADD45A-mediated p38/MAPK signaling pathway. Bioengineered. 2022;13(5):12583–97.
41. Zhang Y, Liao Y, Chen C, Sun W, Sun X, Liu Y, et al. p38-regulated FOXC1 stability is required for colorectal cancer metastasis. J Pathol. 2020;250:217–30.
42. Kumar B, Koul S, Petersen J, Khandrika L, Hwa JS, Meacham RB, Wilson S, Koul HK. p38 mitogen-activated protein kinase-driven MAPKAPK2 regulates invasion of bladder cancer by modulation of MMP-2 and MMP-9 activity. Cancer Res. 2010;70:832–41.
43. Limoge M, Safina A, Truskinovsky AM, Aljahdali I, Zonneville J, Gruevski A, Arteaga CL, Bakin AV. Tumor p38 MAPK signaling enhances breast carcinoma vascularization and growth by promoting expression and deposition of protumorigenic factors. Oncotarget. 2017;8:61969–81.
44. Tang J, Wu W, Yang F, Liu L, Yang Z, Liu L, et al. Marine sponge-derived smenospongine preferentially eliminates breast cancer stem-like cells via p38/AMPKalpha pathways. Cancer Med. 2018;7:3965–76.
45. Yu-Lee LY, Yu G, Lee YC, Lin SC, Pan J, Pan T, Yu KJ, Liu B, Creighton CJ, Rodriguez-Canales J, et al. Osteoblast-secreted factors mediate dormancy of metastatic prostate Cancer in the bone via activation of the TGFbetaRIII-p38MAPK-pS249/T252RB pathway. Cancer Res. 2018;78:2911–24.
46. Wang LZ, Ramírez J, Yeo W, Chan MY, Thuya WL, Lau JY. Glucuronidation by UGT1A1 is the dominant pathway of the metabolic disposition of belinostat in liver cancer patients. PLoS ONE. 2013;9(1):e54522.
47. Finnegan E, Ding W, Ude Z, Terer S, McGivern T, Blümel AM, Kirwan G, Shao X, Genua F, Yin X, Kel A, Fattah S, Myer PA, Cryan SA, Prehn JHM, O'Connor DP, Brennan L, Yochum G, Marmion CJ, Das S. Complexation of histone deacetylase inhibitor belinostat to Cu (II) prevents premature metabolic inactivation in vitro and demonstrates potent anti-cancer activity in vitro and ex vivo in colon cancer. Cell Oncol (Dordr). 2024;47(2):533–53.
48. Pradyuth KS, Salunkhe SA, Singh AK, Chitkara D, Mittal A. Belinostat loaded lipid-polymer hybrid nanoparticulate delivery system for breast cancer: improved pharmacokinetics and biodistribution in a tumor model. J Mater Chem B. 2023;11(45):10859–72.
49. Balasubramaniam S, Redon CE, Peer CJ, Bryla C, Lee MJ, Trepel JB, Tomita Y, Rajan A, Giaccone G, Bonner WM, Figg WD, Fojo T, Piekarz RL, Bates SE. Phase I trial of belinostat with cisplatin and etoposide in advanced solid tumors, with a focus on neuroendocrine and small cell cancers of the lung. Anticancer Drugs. 2018;29(5):457–65.
50. Xu K, Ramesh K, Huang V, Gurbani SS, Cordova JS, Schreibmann E, Weinberg BD, Sengupta S, Voloschin AD, Holdhoff M, Barker PB, Kleinberg LR, Olson JJ, Shu HG, Shim H. Final report on clinical outcomes and Tumor recurrence patterns of a pilot study assessing efficacy of Belinostat (PXD-101) with chemoradiation for newly diagnosed Glioblastoma. Tomography. 2022;8(2):688–700.

Publisher's note